

# Effect of Diapycnal Mixing on Climatic Characteristics of the Laptev Sea in the Ice-Free Period

B. A. Kagan<sup>1</sup>, E. V. Sofina<sup>1, 2, ✉</sup>

<sup>1</sup>Shirshov Institute of Oceanology, Russian Academy of Sciences, Moscow, Russian Federation

<sup>2</sup>Russian State Hydrometeorological University, Saint-Petersburg, Russian Federation

✉ sojjina\_k@mail.ru

## Abstract

**Purpose.** The present study is aimed at evaluating the role of diapycnal mixing conditioned by the dissipation of baroclinic tide energy, in formation of climatic characteristics of the Laptev Sea in summer period.

**Methods and Results.** The sea dynamics with and without tidal forcing is reproduced using the high-resolution 3D finite element model. Spatial resolution of the unstructured grid varied from 1 to 18 km. The wind and thermohaline (seawater temperature and salinity restoring to the specified values on the sea surface) forcings, as well as the sea level at the domain open boundary, are set by the climatic affects corresponding to the summer (July, August) ice-free period in the Laptev Sea. The tidal forcing is set by an indirect method: the diapycnal diffusion coefficient defined, in accordance with the approximation of “weak interaction” of turbulence of various origins, by solving the problem on the baroclinic tide dynamics, is added to the vertical turbulent diffusion coefficient controlled by the wind and thermohaline forcings.

**Conclusions.** The changes in seawater temperature and salinity induced by diapycnal mixing, having been compared to the climatic characteristics as such show that, as a rule, they (especially, their extremal values) are well-detectable, and that their ignoring is not always acceptable. This is confirmed by the average (over the tidal cycle and over the area of the identified sea zone differing from the others by depth) vertical profiles of the uncorrected and corrected (due to the internal tidal wave effects) vertical turbulent mixing coefficients. The profiles differ from one another, if not in the entire sea, then at least within ~ 40% of its volume.

**Keywords:** internal waves, tide, climatic characteristics, turbulent mixing, the Laptev Sea

**Acknowledgments:** the work was carried out within the framework of the state assignment of Shirshov Institute of Oceanology, Russian Academy of Sciences, on theme No. FMWE-2021-0014.

**For citation:** Kagan, B.A. and Sofina, E.V., 2022. Effect of Diapycnal Mixing on Climatic Characteristics of the Laptev Sea in the Ice-Free Period. *Physical Oceanography*, 29(2), pp. 204-219. doi:10.22449/1573-160X-2022-2-204-219

**DOI:** 10.22449/1573-160X-2022-2-204-219

© B. A. Kagan, E. V. Sofina, 2022

© Physical Oceanography, 2022

*To the memory of Sergej Zilitinkevich*

## Introduction

We are aware of only two publications, which are involved in the evaluation of changes in climatic characteristics under diapycnal mixing action induced by the dissipation of baroclinic tides [1, 2]. They are based both on *in situ* sea measurement data and on a comparison of model profiles of the average (over the tidal cycle and over the sea area) coefficients of vertical turbulent and diapycnal diffusion induced by non-tidal (wind + thermohaline + conditioned mass transfer with neighboring water bodies) and purely tidal forcing. Naturally,



the conclusions obtained in these works regarding the importance of changes in climatic characteristics in the sea caused by the baroclinic tide dissipation can be considered as tentative until new empirical information becomes available. Since, however, the appearance of any numerous data of direct measurements in the sea in the near future is hardly possible, the aim of the present paper is to evaluate the role of tides in the formation of the climatic characteristics of the sea using the results of high-resolution modeling and applying the indirect method of describing the baroclinic tidal energy dissipation proposed in [2].

### **An indirect method to describe the effects of internal tidal waves (ITW) and the model used**

Let us dwell briefly on what underlies the indirect method of describing diapycnal diffusion. Explanation of its occurrence mechanism is as follows: it is assumed that diapycnal diffusion owes its origin not to orographic resistance, as was considered in [3], but to the baroclinic tidal energy dissipation, which enters into the expression for the diapycnal diffusion coefficient [4]. Adding the uncorrected vertical turbulent diffusion coefficient controlled by non-tidal forcings to the diapycnal diffusion coefficient makes it possible to estimate the corrected vertical turbulent diffusion coefficient (taking into account the ITW effects). The justification is the “weak interaction” approximation [5]. According to it, if the difference between the characteristic frequencies and spatial scales of turbulence of different origin is sufficiently large, then nonlinear interactions between its individual components can be neglected, approximately assuming them to be additive, although these turbulence components themselves are strongly nonlinear. Solution to the original initial-boundary value problem characterizing the sea climate is sought in the following sequence: first, two auxiliary problems are solved, one corresponding to non-tidal forcings and the other describing the ITW dynamics and energy in the sea under the purely tidal forcing action. From the solution to the first problem, the corresponding uncorrected vertical turbulent diffusion coefficient is found; from the solution to the second problem, the average (for a tidal cycle) diapycnal diffusion coefficient is obtained. Then the uncorrected vertical turbulent diffusion coefficient is corrected by summation with the average local diapycnal diffusion coefficient, after which the equations of sea hydrothermodynamics with the corrected vertical turbulent diffusion coefficient are integrated until the solution reaches the quasi-stationary regime. Comparison of two solutions obtained with and without allowance for ITW effects gives an idea of tidal changes in climatic characteristics in the sea. Here and below, tidal changes in climatic characteristics are understood as changes caused by diapycnal diffusion determined by the ITW effects. The advantage of this description method is rejection of two *a priori* assumptions adopted in [3], namely: invariance in the horizontal plane of the vertical distribution of the baroclinic tidal energy dissipation and fixing the vertical scale of dissipation degeneracy (setting it equal to the value found in the Brazilian Basin), as is done when determining dissipation in terms of orographic resistance. Both assumptions are debatable, bearing in mind the dissipation structure patchiness in the ocean.

It should be noted that all studies of the considered problem so far have dealt mainly with oceanic scales. Regional studies of this kind have not been carried out, except perhaps for those related to the Barents and Kara Seas in [1, 2]. With this in mind, the present work can either confirm the conclusions made in [1, 2] or refute them. To achieve this aim, a three-dimensional finite element hydrostatic model QUODDY-4 [6] was used. We will be limited to listing of the model equations used and describing the special procedure adopted in the model for determining the baroclinic pressure gradient and boundary conditions on the free sea surface and bottom (or rather, at the calculated level closest to the bottom). The present work also lists the empirical information sources used.

The model includes the so-called two-dimensional generalized wave-form continuity equation for free-surface level disturbances, primitive equations of motion written in the hydrostatic and Boussinesq approximations, evolution equations for seawater temperature and salinity and turbulence characteristics (turbulence kinetic energy (TKE) and turbulence scale), a three-dimensional continuity equation used to determine the vertical velocity and the equation of hydrostatics and the seawater state. Evolutionary equations for the horizontal velocity, seawater temperature and salinity and turbulence characteristics after transferring the terms characterizing advection and horizontal turbulent diffusion to the previous time step are solved as a system of non-stationary one-dimensional (vertically) inhomogeneous differential equations.

The adopted model uses a special procedure for determining the baroclinic pressure gradient. Its essence is the seawater density at a fixed horizon interpolated from the  $\sigma$ -coordinate grid to the  $z$ -coordinate grid, after which the baroclinic pressure gradient is calculated on the  $z$ -coordinate grid and then interpolated back to the  $\sigma$ -coordinate grid, where vertical integration of the model equations is carried out.

Boundary conditions for the TKE on the free surface and the calculated level closest to the bottom are given by the Dirichlet condition, which follows from the approximate equality between the production and TKE dissipation when the turbulence scale is approximated by law of the wall and relates the kinetic energy of turbulence to the square of the friction velocity. The boundary values of the turbulence scale are also found there from law of the wall. The vertical momentum flux at the water–air interface required to determine the horizontal velocity is expressed in terms of the momentum flux in the atmospheric near layer, which is parameterized by a quadratic drag law with a drag coefficient equal to  $1.3 \times 10^{-3}$ . The momentum flux in the bottom layer of the sea is also parametrized. The drag coefficient in this case is assumed to be  $5.0 \times 10^{-3}$ . The horizontal turbulent diffusion coefficients are calculated using the well-known Smagorinsky formula.

Wind and thermohaline forcings, as well as the sea level at the open boundary of the computational domain, are set as climatic ones, corresponding to the summer (July, August) ice-free period in the Laptev Sea. The wind field in the near layer of the atmosphere is taken from the ERA-Interim reanalysis of atmospheric data in the Arctic, now recognized as the best of the 7 available reanalysis products [7]. The sea surface level at the domain open boundary is set according to the CNES-CLS09 global ocean mean dynamic topography, supplemented by satellite

altimetry data and *in situ* measurements [8]. Seawater temperature and salinity on the free sea surface are determined using restoring boundary conditions. According to them the normalized heat and salt fluxes on the free sea surface are considered to be proportional to the differences in climatic and predicted values of the variables with a proportionality coefficient that has the meaning of the reverse restoration time. The latter is assumed to be the same for the seawater temperature and salinity and equal to  $10^5$  s, i.e., according to [9], the recovery of the predicted temperature and salinity values to their climatic values is considered strong. The climatic values of the variables are taken from the digital atlas of the Arctic [10], the heat and salt fluxes at the calculated level closest to the bottom are assumed to be zero. The sea is considered to be stratified and free of sea ice and river runoff, making it unnecessary to consider their effects.

Horizontal resolution of the finite element grid is taken to be 5 km on average over the sea area. A terrain-following coordinate is used. The sea column is divided into 40 layers (variable length in depth), thickening in the surface and near-bottom boundary layers. Time step is set as 24 s. The need to select such a time step is dictated by the solution of evolutionary equations for the horizontal velocity, seawater temperature and salinity and turbulence characteristics as a system of non-stationary one-dimensional (vertically) inhomogeneous differential equations. Depths are taken from the IBCAO data bank. The other model parameters are set the same as in its original version [6].

The diapycnal diffusion coefficient required to implement the indirect method of taking into account tidal forcing is set according to the results of [11].

### Simulation results

Starting the discussion of the simulation results, it should be noted that ITW-induced tidal changes in climatic characteristics in the sea cover, as a rule, the entire sea (Fig. 1–7), in contrast to expectations, according to which they do not penetrate beyond the critical latitude (where the tidal and inertial frequencies coincide; in the present case, for wave  $M_2$  the critical latitude equals  $74.5^\circ\text{N}$ ). In other words, the ITW existence domain as freely propagating waves is limited by the critical latitude. Here, ITWs disintegrate (decay) into packets of nonlinear short-period internal waves (NIWs). Generally speaking, reflection of ITW from the critical latitude is also possible. NIWs are not fully reproduced by any tidal model (including the one used here), so that they can propagate only from their generation site, and the existence of tidal changes cannot be associated with them. Then the question arises, what caused the NIWs at supercritical latitudes? It can be assumed, remaining within the framework of the classical theory of tide dynamics, that either a partial ITW disintegration occurs at the critical latitude and, consequently, the existence of degenerate ITWs at supercritical latitudes, or a complete ITW disintegration and, therefore, the existence of some still unidentified ITW generation sites at supercritical latitudes, as evidenced by the analysis of SAR images of the sea surface (see, for example, [12]). The existence of quasi-inertial internal waves at supercritical latitudes neither seems impossible\*.

---

\* Cherkesov, L.V., 1976. *Hydrodynamics of Surface and Internal Waves*. Kyiv: Naukova Dumka, 364 p. (in Russian).

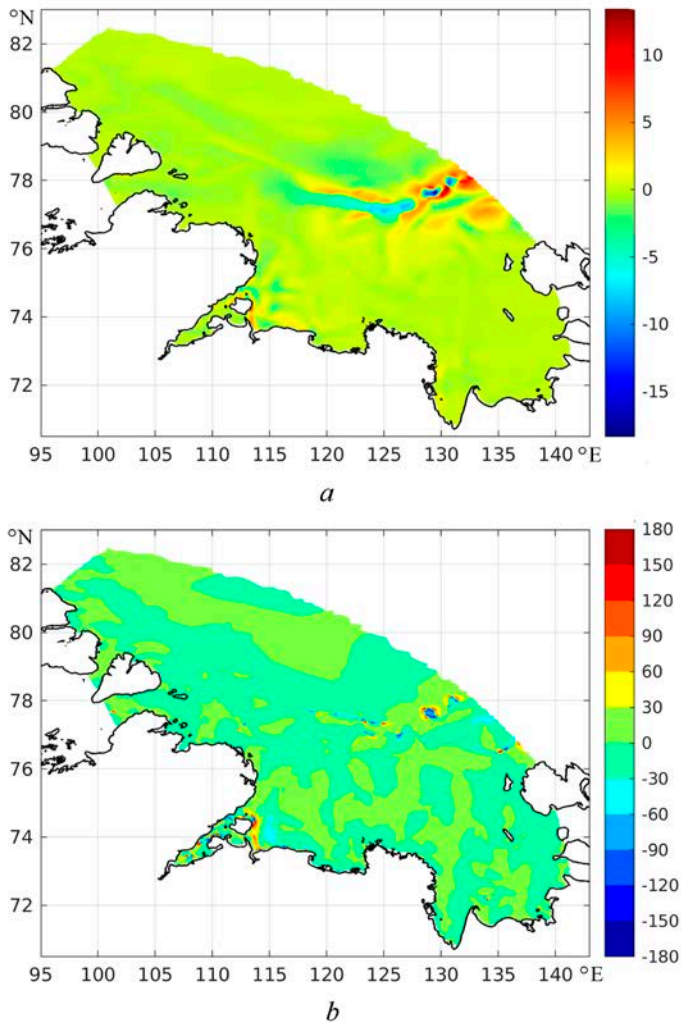


**Fig. 1.** Tidal changes of magnitude (m/s) (a) and direction (°) (b) of the stationary current resulting velocity in the sea surface layer

However, in the second case, it will be necessary to explain which waves are the source of multiple ITW generation at supercritical latitudes. To understand this, it is first of all necessary to solve one more auxiliary problem – to prove that the results obtained are not model-dependent. Until this problem is solved, the results presented can be taken as indicative, intended for estimating the orders of magnitude of the characteristics of interest to us. The results of high-resolution ITW modeling in the Laptev Sea given in [13] can serve as an indirect confirmation of the foregoing, and the results of field measurements presented in [14–17] directly confirm this. Further it will be assumed that a possible explanation for the causes of tidal changes in climatic characteristics in the sea is the existence of a quasi-stationary residual tidal circulation, which is due to the nonlinear interaction of degenerate ITWs at supercritical latitudes. This is the first

circumstance to which the attention should be drawn to. The second is that the average (over the tidal cycle and over the sea area) tidal changes in the magnitude and direction of the resulting velocities of stationary currents in the surface layer of the sea (Fig. 1) are  $-0.1$  cm/s and  $-0.4^\circ$ , respectively, and only on the continental slope in the northern part of the continental slope ( $77.75^\circ\text{N}$ ,  $130.52^\circ\text{E}$ ), they reach higher values (maximum  $13.4$  cm/s and  $8.6^\circ$ ). The same can be said about the resulting velocities in the bottom sea layer (Fig. 2) with the only difference that now the tidal changes in the velocity magnitude at the same point are equal to  $13.1$  cm/s, direction  $-3.8^\circ$ . As can be seen, the differences in the tidal changes in the resulting velocities in these layers are not very large, which implicitly suggests the barotropization of the velocities included in the definition of their tidal changes.

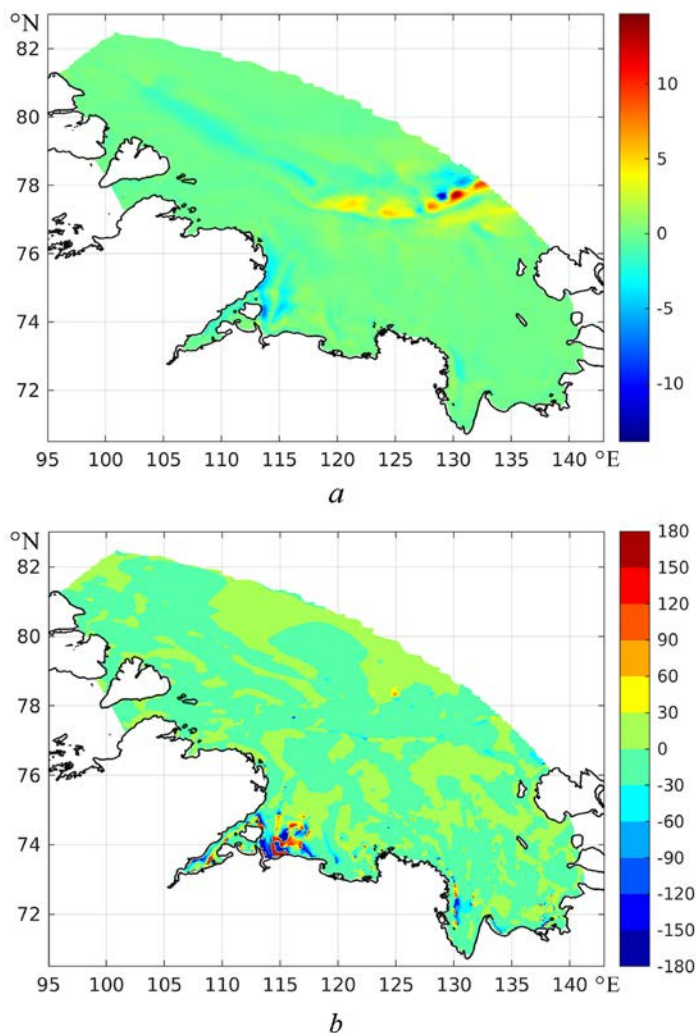


**Fig. 2.** The same as in Fig. 1 for the stationary current resulting velocity in the sea bottom layer

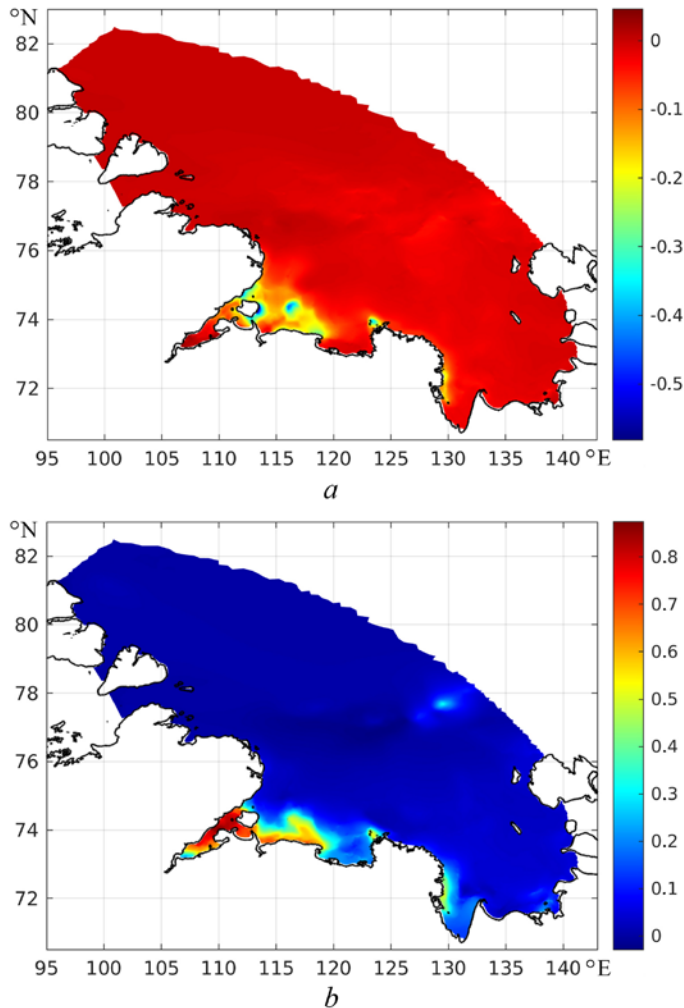


**Fig. 3.** Tidal changes of seawater temperature ( $^{\circ}\text{C}$ ) in the surface (*a*) and bottom (*b*) layers

Fig. 3 shows the fields of tidal changes in seawater temperature in the surface and bottom sea layers. Consequently, a distinctive feature of these fields is an almost homogeneous (in the horizontal plane) structure, covering almost the entire sea, except for the bays in the southeastern part. Tidal temperature changes in the surface layer are  $-0.1$ – $0.0$   $^{\circ}\text{C}$ , in the bottom layer they are  $0.0$ – $0.1$   $^{\circ}\text{C}$ . The most noticeable differences from such a structure are found near the open boundary of the Khatanga Bay in Bolshoy Begichev Island area, where tidal changes reach  $-0.4$   $^{\circ}\text{C}$ , while in the main part of the Anabar Bay they are  $-0.2$   $^{\circ}\text{C}$ . To the east, tidal temperature changes fade everywhere in the Olenek Bay, except for the vicinity of its eastern coast, and then, in the form of a narrow strip bordering the coast of the mainland, are observed near the western coast of the Buor-Khaya Bay.

In the bottom layer, the most noticeable tidal changes in seawater temperature can be detected in the main part of the Khatanga Bay to the northern coast of Bolshoi Begichev Island and further in the form of a narrow strip adjacent to the coast of the mainland; they cover the Nordvik Bay, as well as the Anabar and Oleneksky Bays. At the same time, tidal temperature changes gradually decrease eastward. At the Khatanga Bay boundary, they are 0.7–0.8 °C, they have the same order of magnitude in the Nordvik Bay, then decrease to 0.5–0.6 °C in the Anabar Bay and further to the east in the Oleneksky Bay reach 0.4 °C, and in the western part of the Buor-Khaya Bay again slightly increase to 0.5 °C. We should emphasize the widespread increase in tidal temperature changes in the bottom layer, especially in the Khatanga and other bays listed above, in comparison with the surface layer.

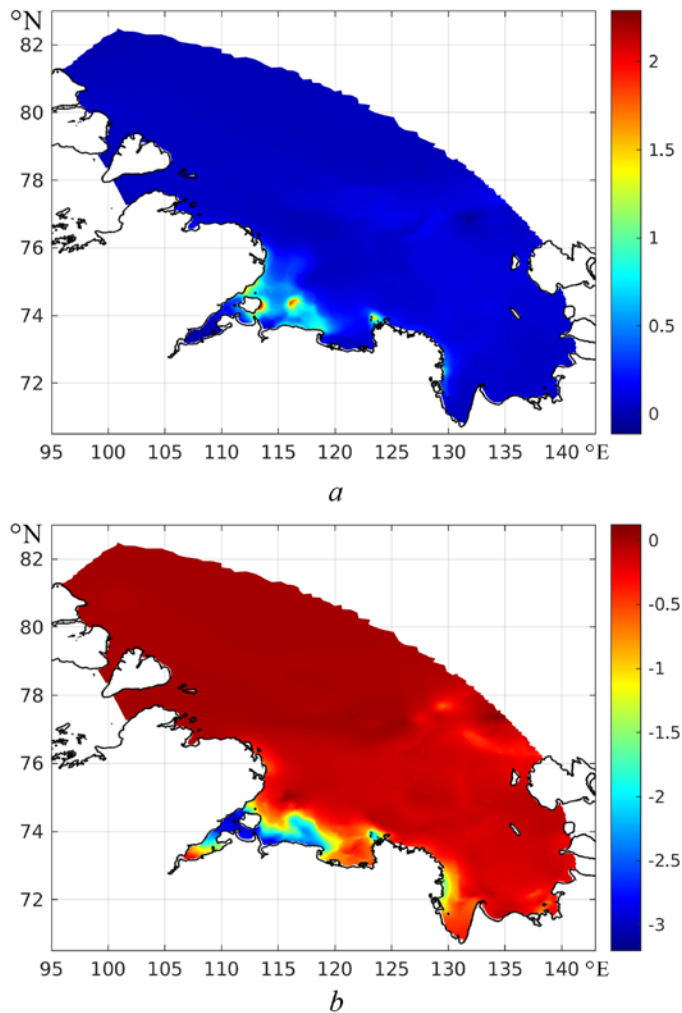


**Fig. 4.** The same as in Fig. 3 for seawater salinity (‰)



The presence of an extensive structure with almost uniform (in the horizontal plane) tidal changes in seawater salinity is also characteristic of the fields shown in Fig. 4. The only difference is the increase in tidal changes in salinity up to 1.3‰ in the surface layer near the northern coast of Bolshoy Begichev Island, an even stronger decrease to 0.5‰ in the main part of the Khatanga Bay, and the Nordvik Bay; on the contrary, a weaker decrease in tidal changes in salinity to 0.3‰ in the Anabar Bay and, finally, the almost complete disappearance of such changes in the Oleneksky and Buor-Khaya Bays. This applied mainly to the surface layer. In the near-bottom layer, tidal changes in salinity are converted from the positive ones in the surface layer to the negative ones. At the same time, in the Khatanga, Nordvik and Anabar Bays, their values are  $-2.5 \dots -2.0$ ‰, then further to the Oleneksky Bay they increase to  $-0.7$ ‰, after which they decrease again to  $-2.0$ ‰ at the eastern boundary of the Oleneksky Bay and  $-1.5$ ‰ and less – in the vicinity of the western coast of the Buor-Khaya Bay.

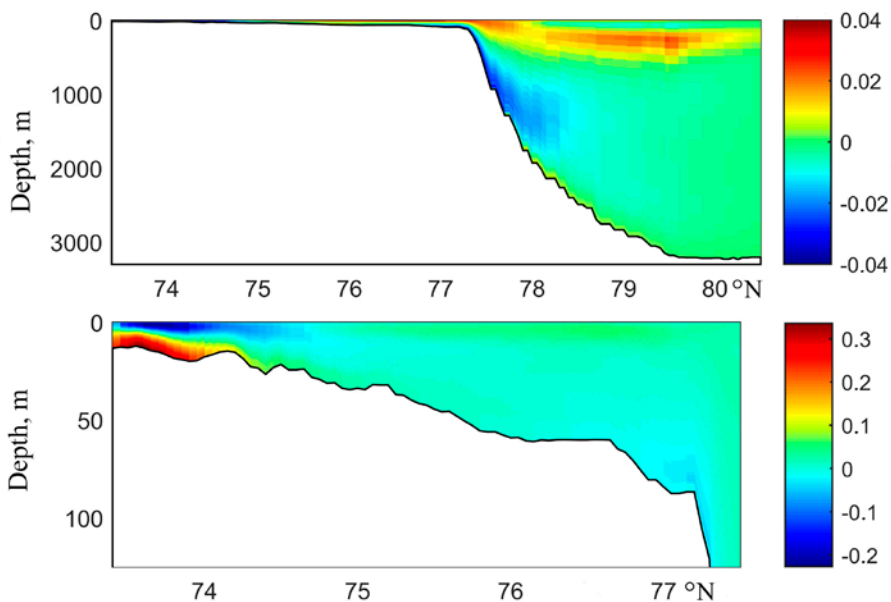


**Fig. 5.** Tidal changes of seawater temperature ( $^{\circ}\text{C}$ ) along the meridional transect  $120^{\circ}\text{E}$ . In the upper fragment, the tidal temperature changes are shown along the entire section, in the lower fragment – along its shallow-water part on the enlarged scale

Fig. 5 and 6 show tidal changes in the seawater temperature and salinity along the  $120^{\circ}\text{E}$  meridian. In the main seawater column, their values reach  $0.03^{\circ}\text{C}$  for temperature and vary within  $-0.05 \dots 0.05$ ‰ for salinity, wedging out with increasing distance to the north. Let us note that the wedging out of tidal changes in seawater temperature and salinity can be caused by ITW degeneration. These figures are interesting in yet another respect, as evidence that the main tidal changes in these variables occur not in the surface layer, but in the lower layers of the sea, including the bottom one. Here, tidal temperature changes in the shallow part of the section are several times greater than in the surface layer, and tidal changes in salinity there also vary within  $0.5 \dots -1.0$ ‰.

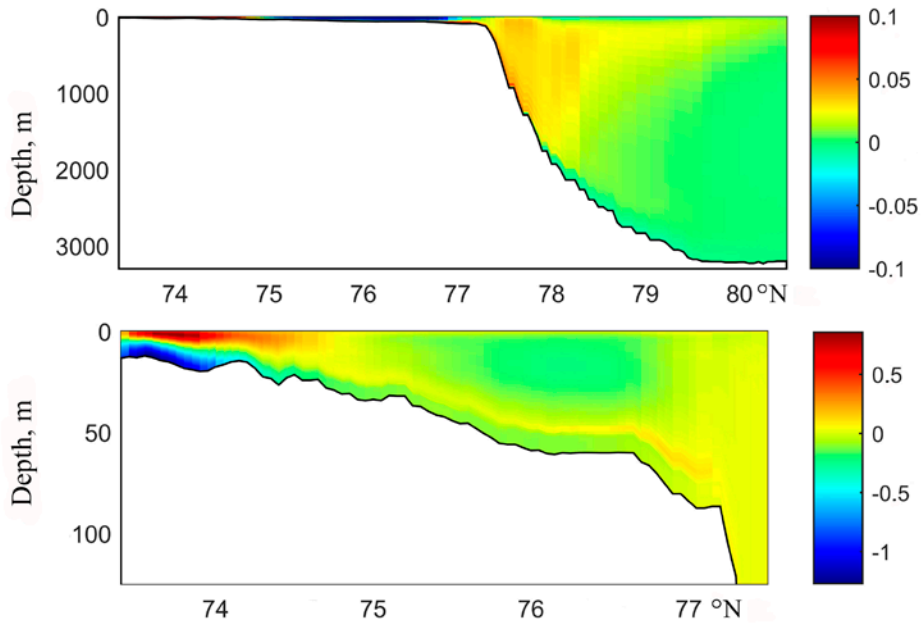


**Fig. 6.** The same as in Fig. 5 for seawater salinity (‰)

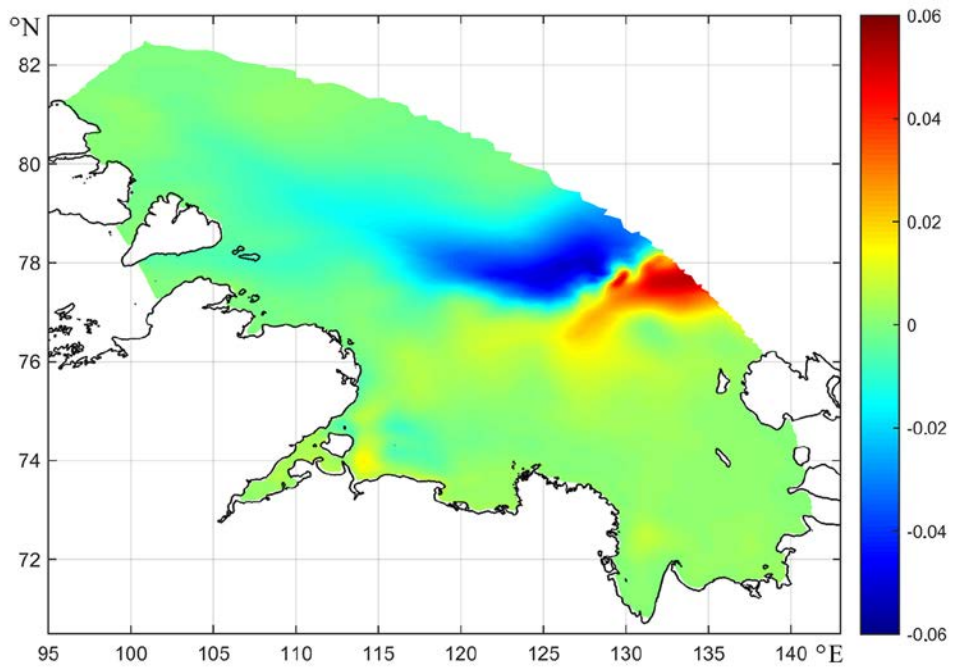


**Fig. 7.** Tidal changes of the sea surface level (m)

Another feature of tidal changes of climatic characteristics in the sea is related to the field of tidal sea level changes (Fig. 7). It has a distinct striped structure, vaguely resembling continental slope outlines. The magnitude of tidal level changes in this structure is  $\pm 0.06$  m, from a drop in level ( $-0.06$  m) in the vicinity of the continental slope to an increase ( $0.04$  m and above) in shallow water east of the continental slope, and remains close to zero values in the western and eastern parts of the sea.

It is known that the Laptev Sea is characterized by the division of depths into two areas – the shallow water (inner shelf) and the deep water (outer shelf). In the first one, vertical turbulent diffusion can propagate to the entire sea column; in the second, which includes the stratified part of the water column, ITW generation can occur, but only up to the critical latitude. As already mentioned, ITWs disintegrate into packets of NIWs, so that ITWs cannot propagate freely at supercritical latitudes. Which of the unidentified waves have such capability is still unknown. It is only known that, near the critical latitude, NIWs differ significantly from ITWs and that, apparently, one of the probable mechanisms for their generation is the one that is inherent in lee waves induced on the leeward side of underwater obstacles [17]. Consequently, at present we have two explanations for the mechanism of NIWs generation at supercritical latitudes. One of them, mentioned above, relates the NIWs to the partial disintegration of ITWs at the critical latitude into packets and subsequent NIWs propagation, as well as degenerate ITWs, which serve as generation sites of other SIWs at supercritical latitudes. The second explanation interprets NIWs as lee waves formed on the downstream side of bottom irregularities such as a shelf edge and an isolated bottom uplift [18]. Such an explanation concretizes the mechanism of NIWs generation, but does not reveal their origin at supercritical latitudes. Which of the explanations presented here is preferable, remains a matter of judgment.

It can be expected that tidal changes in climatic characteristics in the sea appear in both shallow and deep-water areas. However, the expectations are only partially justified: the average (over the tidal cycle and over the sea area) corrected (due to ITW effects) and uncorrected vertical turbulent diffusion coefficients differ from each other by less than an order of magnitude, and only in zone IV (Fig. 8), their discrepancies turn out to be greater in the layer located deeper than the 2,500 m horizon. To make the conclusion about the vertical distribution of the two coefficients clearer, we single out a shallow-water area in the sea with the depths of up to 100 m (zone I), bordering the continental slope area with depths of 100–500 m (zone II), an area adjacent to it from the north with the depths of 500–2,500 m (zone III), and a deep-water area with the depths over 2,500 m (zone IV). In every such region, the average corrected and uncorrected vertical turbulent diffusion coefficients are determined. From Fig. 9 it follows that the ITW-induced discrepancies in the values of these coefficients are concentrated mainly in the lower layers, the volume of which, relative to the sea volume as a whole, is  $\sim 40\%$ . The noted circumstance gives reason to believe that the greatest tidal changes in climatic characteristics, in particular the seawater temperature and salinity, are in the lower, and not in the upper layers of the sea.

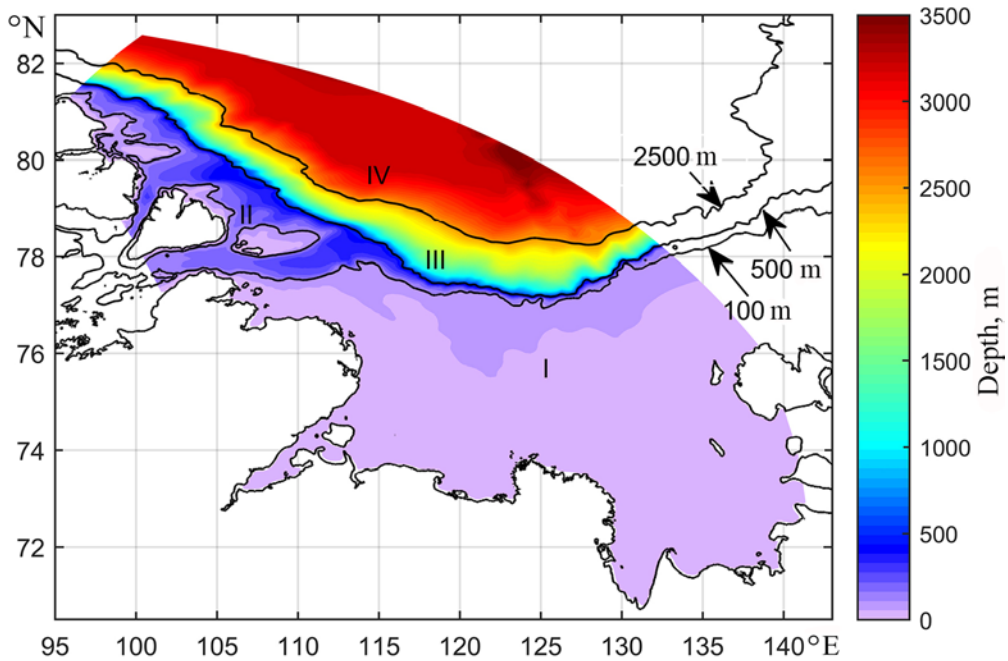


**Fig. 8.** Bottom topography and the specific zones with different depths

Now that estimates of tidal changes in temperature and salinity in the sea have been obtained, the problem of comparing the simulation results with observational data appears. However, its implementation is difficult due to the lack of mass measurements of some of the climatic characteristics in the sea. Of the 5 such characteristics (magnitude and direction of the resulting velocity of stationary currents, seawater temperature and salinity, free surface sea level), only temperature and salinity have the necessary data. Comparison of the rest due to the paucity of observational data has to be abandoned. According to the simulation results, the average (over the tidal cycle and over the sea area) tidal changes in seawater temperature and salinity, defined as the difference between their predicted values taking into account the ITW effects and the reference values controlled only by non-tidal forcings and thus not taking into account the ITW effects, are equal to  $0.02\text{ }^{\circ}\text{C}$  and  $0.10\text{‰}$  in the surface layer and  $0.05\text{ }^{\circ}\text{C}$  and  $-0.20\text{‰}$  in the bottom layer. Their comparison with the corresponding climatic characteristics shows that they are commensurate with the same climatic characteristics for temperature and much less for salinity. It follows that the conventional disregard for tidal changes in temperature and salinity in the sea is justified for salinity and has no basis for seawater temperature. Whether it is generally the case, needs to be determined. See below for possible reasons for the appearance of such estimates of tidal changes in seawater temperature and salinity.

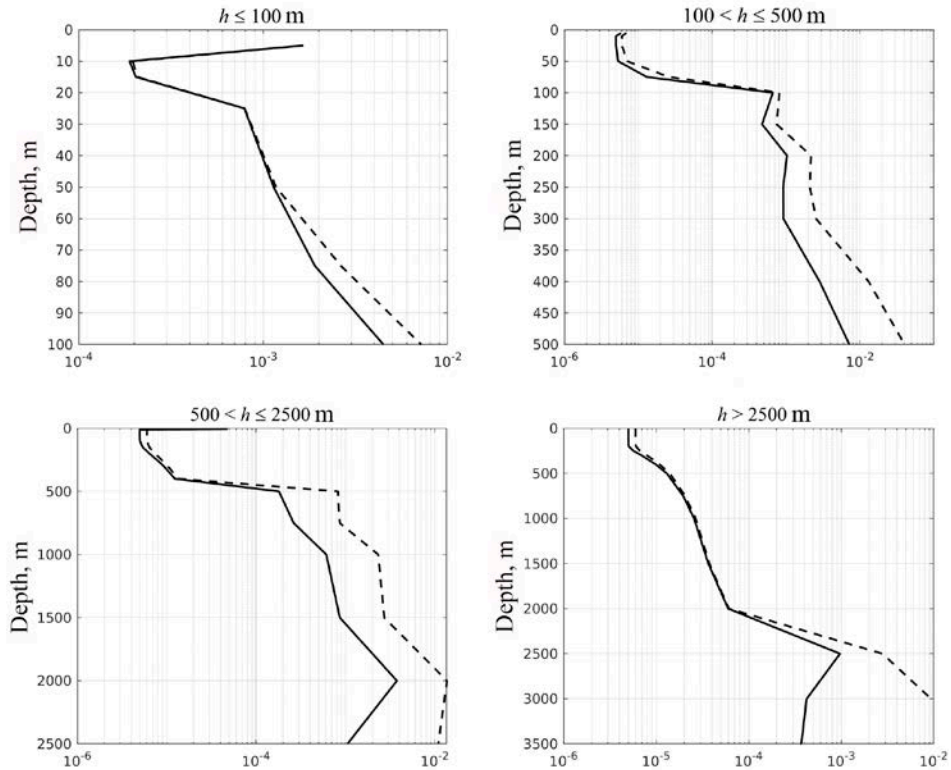


**Fig. 9.** Vertical profiles of the average (over the area of any specific zone) values of the non-corrected (solid line) and corrected (dashed line) (due to the ITW effects) coefficients of vertical turbulent diffusion ( $\text{m}^2/\text{s}$ )

Now we are to consider how the observed and model tidal changes in seawater temperature and salinity differ from each other. Here we are faced with the need to estimate the reference values of temperature and salinity from observational data. The point is that the observational data bear the imprints of all the considered forcings, including the tidal forcing, while only non-tidal forcings are responsible for the reference values. Indeed, the observational data alone is not enough to estimate reference values of seawater temperature and salinity. They must first be exposed to the procedures for revealing hidden periodicity or traditional harmonic analysis, then it is necessary to eliminate the selected tidal harmonic. There is another possibility: to involve the results of the simulation. We preferred the second option. Acting in this way, it has been found that the observed and model values of the variables differ from each other by no more than  $0.1\text{ }^\circ\text{C}$  for temperature and  $0.7\text{‰}$  for salinity, i.e., the discrepancies between them are acceptable.

Note one more detail: it is required to understand the reasons for the appearance of relatively small model tidal changes in the seawater temperature and salinity. Among them, there may be either inevitable errors in estimating the reference values of temperature and salinity based on the simulation results, or

averaging the initial fields over the sea area, leading to compensation for tidal changes in variables with opposite signs, or, finally, the unrepresentativeness of the found estimates of tidal changes in the Laptev Sea temperature and salinity, compared to those predicted in other marginal seas.

Comparatively small model values of tidal changes in the seawater temperature and salinity are most likely the consequences of averaging over the sea area, which compensates for tidal changes in variables with opposite signs. That this is the case can be verified by referring to their maximum values. For example, the maximum tidal temperature change ( $0.87\text{ }^{\circ}\text{C}$ ) in the bottom layer is observed at the point with coordinates  $73.97^{\circ}\text{N}$ ,  $109.92^{\circ}\text{E}$ , while the maximum tidal change in salinity in the same layer ( $-3.20\text{‰}$ ) is at the point with coordinates  $74.40^{\circ}\text{N}$ ,  $111.80^{\circ}\text{E}$ . Here and below, the signs of tidal changes depend entirely on the difference between the variables induced by different forcings: if it is positive or negative, the sign of the tidal change in temperature and salinity will be the same. Further, local tidal changes of the same variables in the surface layer are smaller ( $-0.12\text{ }^{\circ}\text{C}$  and  $0.21\text{‰}$  versus  $0.87\text{ }^{\circ}\text{C}$  and  $-2.75\text{‰}$ ) in absolute value in comparison with the given maximum tidal changes in temperature and salinity in the bottom layer at the point with coordinates  $73.97^{\circ}\text{N}$ ,  $109.92^{\circ}\text{E}$ . Limiting the observations to only the second pair of estimates as the largest in the same sense, it is seen that in relative units, normalized to the value of these variables in the bottom layer, local tidal changes are  $\sim 100\%$  for temperature and  $\sim 10\%$  for salinity and that, consequently, predictions and calculations of extreme tidal changes in temperature and salinity in the sea can be improved by taking into account the ITW effects.

### Conclusion

Now we are to summarize the results of the work carried out. Using a high-resolution version of a three-dimensional finite element hydrostatic model QUODDY-4, tidal changes in the magnitude and direction of the resulting velocities of stationary currents in the Laptev Sea surface and bottom layers, the seawater temperature and salinity in the same place, the level of the free surface and vertical distributions of tidal changes in temperature and salinity are reproduced along the meridional section  $120^{\circ}\text{E}$ . The simulation results show that the average (over the tidal cycle and over the sea area) tidal changes in the first 9 climatic characteristics in the sea are, respectively:  $-0.1\text{ cm/s}$  and  $-0.4^{\circ}$  in the surface layer;  $0.0\text{ cm/s}$  and  $-2.2^{\circ}$  in the bottom layer;  $-0.02$  and  $0.05\text{ }^{\circ}\text{C}$  for temperature and  $0.10$  and  $-0.20\text{‰}$  for salinity in the same place;  $-0.002\text{ m}$  for sea level. It has also been found that the simulation results indicate an increase in tidal changes in temperature and salinity in the near-bottom layer compared to the surface. This fact is confirmed by comparing the vertical profiles of the corrected (due to ITW effects) and uncorrected vertical turbulent diffusion coefficients determined, respectively, by all the considered forcings, including the tidal one. Estimating the average (over the sea area) and extreme tidal changes in temperature and salinity, we are convinced that the generally accepted ignorance of tidal changes in the seawater temperature and salinity is only partially justified: it is true for average (over the sea area) values and not true for extreme ones. The latter, as applied to the Laptev Sea, are  $\sim 100\%$  for temperature and  $\sim 10\%$  for salinity in relative units. This means that the currently existing methods for

forecasting and calculating extreme values of seawater temperature and salinity in the part of the sea volume, equal to ~ 40% of the total volume, in this case need to be revised.

#### REFERENCES

1. Kagan, B.A. and Sofina, E.V., 2017. A Method of Accounting for Tidal Changes in Regional Climates of a Water Basin under Conditions of an Ice-Free Barents Sea. *Oceanology*, 57(2), pp. 245-252. doi:10.1134/S0001437016060047
2. Kagan, B.A., Sofina, E.V. and Timofeev, A.A., 2019. The Tidal Effect on Climatic Characteristics of the Kara Sea in the Ice-Free Period. *Izvestiya, Atmospheric and Oceanic Physics*, 55(2), pp. 188-195. doi:10.1134/S0001433819020087
3. Jayne, S.R. and St. Laurent, L.C., 2001. Parameterizing Tidal Dissipation over Rough Topography. *Geophysical Research Letters*, 28(5), pp. 811-814. doi:10.1029/2000GL012044
4. Osborn, T.R., 1980. Estimates of the Local Rate of Vertical Diffusion from Dissipation Measurements. *Journal of Physical Oceanography*, 10(1), pp. 83-89. doi:10.1175/1520-0485(1980)010<0083:EOTLRO>2.0.CO;2
5. Zaslavsky, G.M. and Sagdeev, R.Z., 1988. *Introduction to Nonlinear Physics*. Moscow: Nauka, 368 p. (in Russian).
6. Ip, J.T.C. and Lynch, D.R., 1995. *Comprehensive Coastal Circulation Simulation using Finite Elements: Nonlinear Prognostic Time-Stepping Model: QUODDY3 User's Manual*. Hanover, New Hampshire, USA: Thayer School of Engineering, Dartmouth College, 45 p.
7. Lindsay, R., Wensnahan, M., Schweiger, A. and Zhang, J., 2014. Evaluation of Seven Different Atmospheric Reanalysis Products in the Arctic. *Journal of Climate*, 27(7), pp. 2588-2606. doi:10.1175/JCLI-D-13-00014.1
8. Rio, M.H., Guinehut, S. and Larnicol, G., 2011. New CNES-CLS09 Global Mean Dynamic Topography Computed from the Combination of GRACE Data, Altimetry, and In Situ Measurements. *Journal of Geophysical Research: Oceans*, 116(C7), C07018. doi:10.1029/2010JC006505
9. Jayne, S.R., 2009. The Impact of Abyssal Mixing Parameterizations in an Ocean General Circulation Model. *Journal of Physical Oceanography*, 39(7), pp. 1756-1775. doi:10.1175/2009JPO4085.1
10. Environmental Working Group, 1997. *Environmental Working Group Joint U.S.-Russian Atlas of the Arctic Ocean, Version 1*. Boulder, Colorado USA: NSIDC. doi:10.7265/N5H12ZX4
11. Kagan, B.A. and Timofeev, A.A., 2020. The Determination of Baroclinic Tidal Energy Dissipation and Its Related Diapycnal Diffusivity as the First Step in Estimating the Role of Tidal Effects in the Formation of the Laptev Sea's Climatic Characteristics. *Fundamentalnaya i Prikladnaya Gidrofizika*, 13(4), pp. 39-49 (in Russian). doi:10.7868/S2073667320040048
12. Kozlov, I.E., Zubkova, E.V. and Kudryavtsev, V.N., 2017. Internal Solitary Waves in the Laptev Sea: First Results of Spaceborne SAR Observations. *IEEE Geoscience and Remote Sensing Letters*, 14(11), pp. 2047-2051. doi:10.1109/LGRS.2017.2749681

13. Kagan, B.A. and Timofeev, A.A., 2020. High-Resolution Modeling of Semidiurnal Internal Tidal Waves in the Laptev Sea in the Ice-Free Period: Their Dynamics and Energetics. *Izvestiya, Atmospheric and Oceanic Physics*, 56(5), pp. 512-521. doi:10.1134/S0001433820050047
14. Pingree, R.D. and New, A.L., 1995. Structure, Seasonal Development and Sunlight Spatial Coherence of the Internal Tide on the Celtic and Armorican Shelves and in the Bay of Biscay. *Deep Sea Research Part I: Oceanographic Research Papers*, 42(2), pp. 245-284. doi:10.1016/0967-0637(94)00041-P
15. Hsu, M.-K., Liu, A.K. and Liu, C., 2000. A Study of Internal Waves in the China Seas and Yellow Sea Using SAR. *Continental Shelf Research*, 20(4–5), pp. 389-410. doi:10.1016/S0278-4343(99)00078-3
16. Holloway, P.E., Chatwin, P.G. and Craig, P., 2001. Internal Tide Observations from the Australian North West Shelf in Summer 1995. *Journal of Physical Oceanography*, 31(5), pp. 1182-1199. doi:10.1175/1520-0485(2001)031<1182:ITOFTA>2.0.CO;2
17. Rainville, L. and Pinkel, R., 2006. Propagation of Low-Mode Internal Waves through the Ocean. *Journal of Physical Oceanography*, 36(6), pp. 1220-1236. doi:10.1175/JPO2889.1
18. Vlasenko, V., Stashchuk, N., Hutter, K. and Sabinin, K., 2003. Nonlinear Internal Waves Forced by Tides near the Critical Latitude. *Deep Sea Research Part I: Oceanographic Research Papers*, 50(3), pp. 317-338. doi:10.1016/S0967-0637(03)00018-9

*About the authors:*

**Boris A. Kagan**, Chief Researcher, P. P. Shirshov Institute of Oceanology, RAS (36 Nahimovskiy pr., Moscow, 117997, Russian Federation), Dr.Sci. (Phis.-Math.), Professor, **WoS ResearcherID: AAD-1931-2021**, **Scopus Author ID: 7005584755**, **Author ID: 1171**, kagan@ioras.nw.ru

**Ekaterina V. Sofina**, Leading Researcher, P. P. Shirshov Institute of Oceanology, RAS (36 Nahimovskiy pr., Moscow, 117997, Russian Federation), Associate professor, Russian State Hydrometeorological University (79 Voronezhskaya, St., St.Petersburg, 192007, Russia), Ph.D. (Phis.-Math.), **ORCID ID: 0000-0001-9206-8253**, **WoS ResearcherID: E-3920-2014**, **Scopus Author ID: 23111468200**, **Author ID: 169097**, sofjina\_k@mail.ru

*Contribution of the co-authors:*

**Boris A. Kagan** – the problem setting, analysis of the results, writing the text of the article

**Ekaterina V. Sofina** – carrying out the simulations, proceeding the results, constructing maps, editing the text of the article

*The authors have read and approved the final manuscript.*

*The authors declare that they have no conflict of interest.*